

METASTABLE PHASE AND AGE HARDENING IN RAPIDLY-SOLIDIFIED SILVER-RICH Ag-Gd ALLOYS^①

Ning Yuantao

Institute of Precious Metals, Kunming 650221

ABSTRACT The splat foils and spun ribbons of Ag-Gd alloys with 0.08 and 0.03 mm in average thickness were made by hammer-anvil and spinning melt quenching technique, and the cooling rate was determined to be 10^6 and 10^7 K/s, respectively. The metastable solid solubility limit of Gd reached 5.0% ~ 6.0%, and a metastable intermediate phase with hexagonal lattice structure, Ag_3Gd , was found in RS Ag-Gd alloys. A strong solid solution strengthening and age hardening response were observed. The precipitate phase which was responsible for the age hardening was identified to be $\text{Ag}_{51}\text{Gd}_{14}$ equilibrium intermediate phase.

Key words metastable phase age hardening rapidly-solidified Ag-Gd alloy

1 INTRODUCTION

Since the rapid solidification(RS) technique was developed^[1], the metastable extension of solid solubility and the formation of metastable phase have been the subject of much research. In order to develop a new Ag alloy with high strength through RS technology, the metastable phase structure and age hardening in RS Ag-Gd alloys were studied in present paper.

2 EXPERIMENTAL PROCEDURE

A series of binary Ag-Gd alloys were prepared in an arc furnace using pure Ag with 99.999% purity and Gd with 99.9% purity. Two kinds of RS specimens, splat foils and spun ribbons, were made. The splat foils with average thickness 0.08 mm (in range of 0.07~0.09 mm) were made by an arc-melt hammer and anvil technique. The spun ribbons with average thickness 0.03 mm (in range of 0.02~0.04 mm) were made by a spinning technique. The ICP-AES quantitative spectrum analysis was used to measure the Gd concentration of the RS specimens. The lattice parameters of RS Ag-Gd alloys were determined by $\text{CuK}\alpha$ ($\lambda = 0.15406$ nm) X-ray diffraction (XRD) analysis on a D/

max-3B(3 kW) diffractometer. The positions of the diffraction peaks were corrected by an external reference standard. The lattice parameters were calculated from the corrected peak positions via least-squares refinement. No diffraction line of Gd oxide was detected in the diffraction patterns. The microstructure and morphology of RS Ag-Gd alloys were observed in JEM-2000EX TEM.

3 METASTABLE PHASE IN RS Ag-Gd ALLOYS

3.1 Cooling rate

According to the heat flow analysis theory^[1, 2], for effectively perfect contact conditions between metallic melt and chill surface, the cooling rate, ε , at the uncooled boundary equals to

$$\varepsilon = B' / Z^2 \quad (1)$$

where B' is a function of relevant temperature intervals and materials properties and $B' = 10^4 \text{ mm}^2 \text{ K/s}$, Z is the thickness of sample section. The formula can be used to evaluate the cooling rate of RS Ag-Gd foil and ribbon samples, and $\varepsilon = 1.6 \times 10^6 \text{ K/s}$ for foil sample and $1.0 \times 10^7 \text{ K/s}$ for ribbon samples.

The cooling rate can be measured from the secondary dendritic spacing. Fig. 1 shows the

① Received Dec. 7, 1995; accepted Feb. 18, 1996

dendrite formation in RS Ag-Gd₄ alloy ribbon. The measured secondary dendrite spacing (ξ) is about 0.25 mm. According to the power function relationship between ξ and the cooling rate ε , we have

$$\xi = B\varepsilon^{-n} \text{ or } \varepsilon = (B/\xi)^{1/n} \quad (2)$$

Because the cooling characteristics of silver alloy is similar to that of copper alloy. Taking $n = 0.4$ and $B = 160$ for studied RS Ag-RE alloy^[2], then the cooling rate ε was found to be 1.04×10^7 K/s from the Eqn. (2). The measured ε value corresponded completely with that determined by Eqn. (1).



Fig. 1 The dendrite formation of RS Ag-Gd₄ alloy ribbon

3.2 Metastable solid solubility limit

The dependence of the lattice parameter of RS Ag-Gd alloys on Gd concentration is shown in Fig. 2. The atomic radius of Gd (0.179 nm) is 24% larger than that of Ag (0.144 nm), so the lattice parameters of the solid solution increase with the Gd concentration and then keep constant in duplex phase region. The solute concentrations corresponding to the inflexion point

in Fig. 2 are the metastable solid solubility limits, they are 5% Gd for splat foil with lower cooling rate and 6% Gd for spun ribbon with higher cooling rate. Compared with the equilibrium solid solubility (0.95% Gd^[4]), the solid solubility of RS Ag-Gd alloy has large extension. The metastable solid solubility limit determined by the lattice parameter method were tested and verified through microstructure observation. For RS Ag-Gd alloy foil specimen, Ag-Gd₂ and Ag-Gd₄ alloys are single solid solutions (Fig. 3(a), (b)), whereas the particles of second phase have occurred in a small amount in RS Ag-Gd₆ alloy (Fig. 3(c)) and increased obviously in Ag-Gd₈ alloy (Fig. 3(d)). The structure change is in accord with lattice parameter change.

3.3 Metastable intermediate phase

The secondary phase in RS Ag-Gd alloy foils was identified by XRD analysis. The XRD spectrum of Ag-Gd₂ and Ag-Gd₄ alloys was one of single solid solution. When Gd concentration is above 5%, the spectrum of secondary phase occurred. The lattice plane spacing (d_{exp}) and the relative intensity of the diffraction lines for splat Ag-Gd₆ foil are listed in Table 1. These

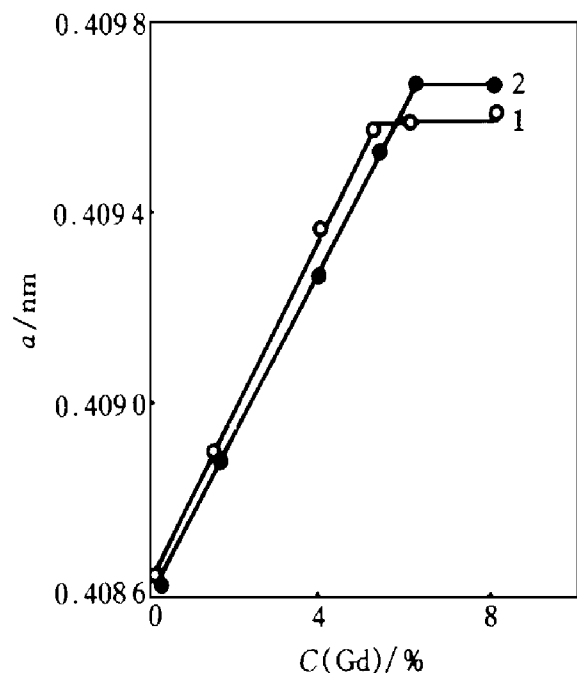


Fig. 2 The lattice parameters, a , vs Gd concentrations for RS Ag-Gd alloy foil and ribbon
1—Foil; 2—Ribbon

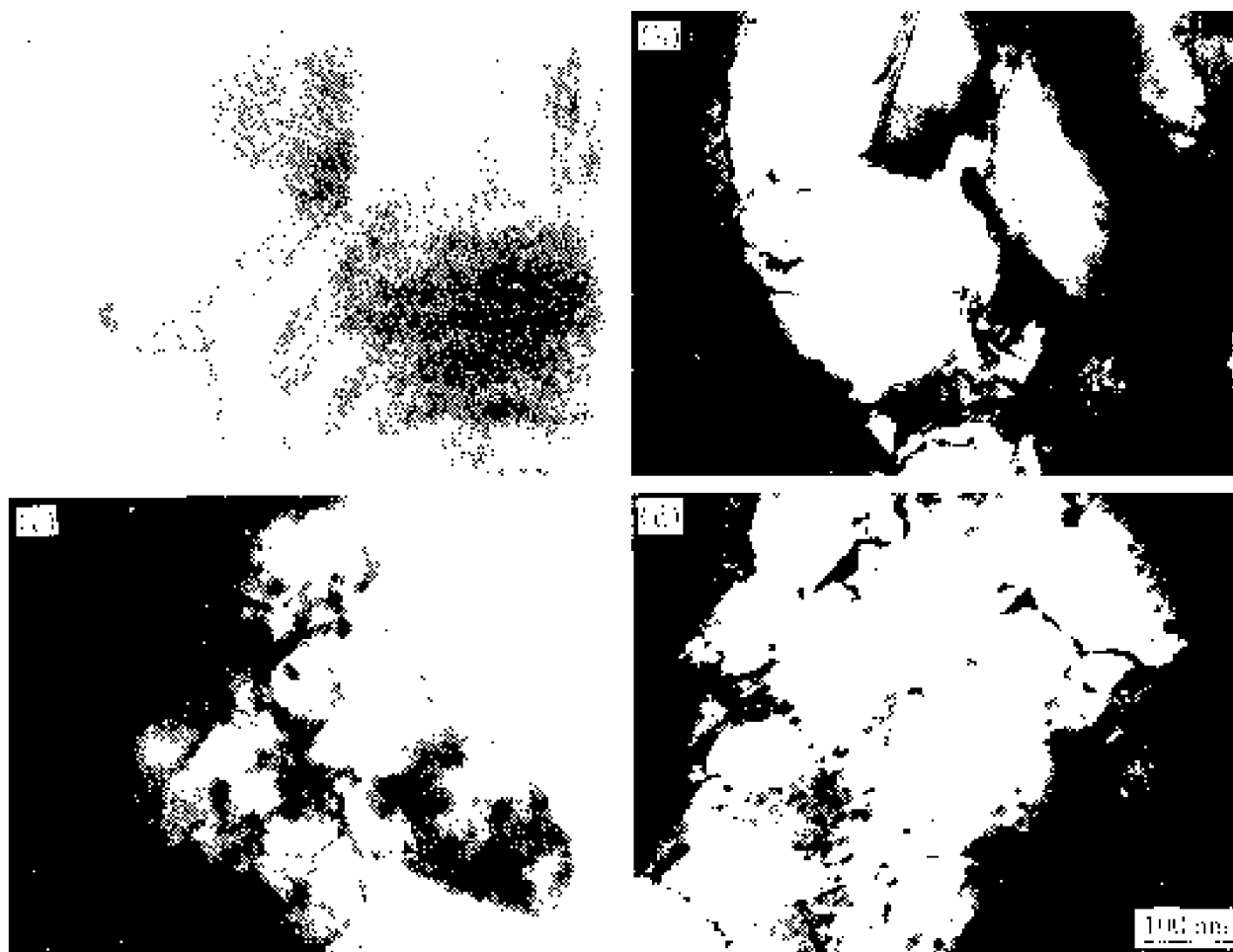


Fig. 3 Microstructure of RS Ag-Gd alloy foils

(a, b) $-\text{Ag-Gd}_2$ alloy, single solid solution (SS);

(c, d) $-\text{Ag-Gd}_6$ and Ag-Gd_8 , SS+ Ag_3Gd

Table 1 A comparison of diffraction data of RS Ag-Gd₆ alloy with those of Ag and Ag₃Gd

RS Ag-Gd ₆ foil			Ag ^[5]			Ag ₃ Gd ^[6]		
$2\theta/^\circ$	d_{exp}/nm	I/I_1	d/nm	I/I_1	hkl	d/nm	I/I_1	hkl
33.08	0.270 5	1				0.273 9	40	040
35.74	0.251	2				0.251	30	230
36.24	0.247 5	4				0.247	100	123
38.02	0.236 4	100	0.236	100	111			
40.64	0.221 8	4				0.221 2	50	223
42.92	0.210 5	2				0.211 8	60	412
44.29	0.204 4	22	0.204 5	40	200			
64.28	0.147 7	12	0.144 5	25	220			
77.26	0.123 3	11	0.123 2	26	311			
81.38	0.118 1	5	0.118 1	12	222			
97.56	0.102 4	1	0.102 2	4	400			
110.74	0.093 6	2	0.093 8	15	331			
114.64	0.091 5	3	0.091 4	12	420			

values coincide completely with that of Ag and Ag_3Gd . It indicated that the splat RS Ag-Gd₆ alloy consists of Ag(Gd) and Ag_3Gd . The proportion of Ag_3Gd increases with Gd concentration in RS Ag-Gd alloy. The Ag_3Gd is an Ag_3Pu -type hexagonal structure with lattice parameters $a = 1.2587 \text{ nm}$, $c = 0.9207 \text{ nm}$ and melting point 975°C ^[5]. In equilibrium state, the first silver-rich intermediate phase is $\text{Ag}_{51}\text{Gd}_{14}$ ^[3], the Ag_3Gd is only the metastable intermediate phase occurred in RS Ag-Gd alloy system. Similarly, the Ag_3RE phase is also found in other RS Ag-RE systems^[4].

4 PHASE STRUCTURE OF Ag-Gd ALLOY RAPIDLY-SOLIDIFIED AND FOLLOWED BY AGEING

4.1 Age hardening of RS Ag-Gd alloys

The maximum solid solubility of Gd in Ag can be extended to 5% ~ 6% from 0.95% equilibrium value through RS technology with cooling rate of $10^6 \sim 10^7 \text{ K/s}$. So, the RS Ag-Gd alloys are the metastable supersaturated solid solution (MSSS) or MSSS+ Ag_3Gd , and have obvious solid solution strengthening and age hardening. Fig. 4 shows the age hardening responses of RS Ag-Gd₄ and Ag-Gd₆ alloy foils. The hardness values at ageing peaks of about 200~250 °C are as high as 2.35 and 2.75 GPa for Ag-Gd₄ and Ag-Gd₆ alloys and increased by about 25% and 18% as compared with that of their corresponding RS states. The hardening response of RS Ag-Gd₆ alloy is over that of RS Ag-Gd₄ alloy due to the higher solid solubility of Gd and the existence of Ag_3Gd metastable phase in RS Ag-Gd₆ alloy, whereas RS Ag-Gd₄ alloy is a single solid solution. In addition, the hardness of the RS alloys is obviously higher than that of the alloys annealed at above 400 °C, because the former is a supersaturated solid solution with finer crystal grains and lattice distortion.

In the age hardening process of RS Ag-Gd alloy, Gd solute was separated from the supersaturated solid solution. So, the lattice parameter of the alloy decreased gradually, as shown in Fig. 5, and reached $a = 0.4087 \text{ nm}$ at 600 °C

which corresponds to that of Ag-Gd_{0.5} alloy. It indicated that the solid solubility of Gd had reached the corresponding equilibrium value.

Fig. 6 shows the microstructure change of RS Ag-Gd₄ alloy in ageing process. In RS Ag-Gd₄ supersaturated solid solution, the fine particles of second phase precipitated out inside the grains of the alloy aged at 150 °C for 30 min which made the hardness increase. At 200 °C aging, a large amount of the second phase particles formed dispersal distribution, and the hardness reached the peak value. At the temperatures

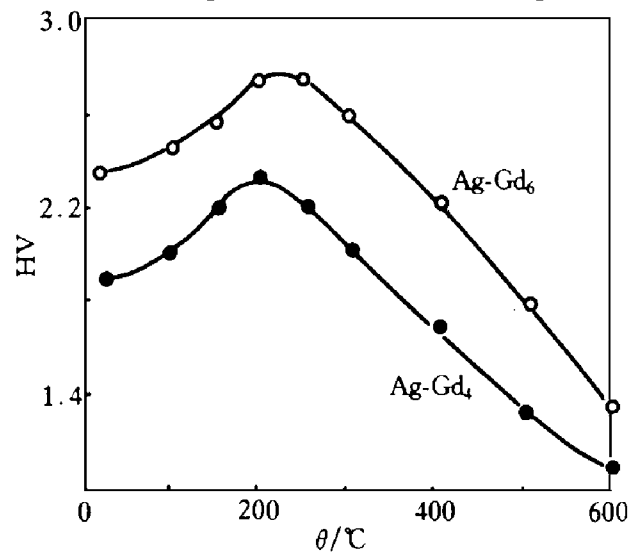


Fig.4 Age response of RS Ag-Gd alloy foils

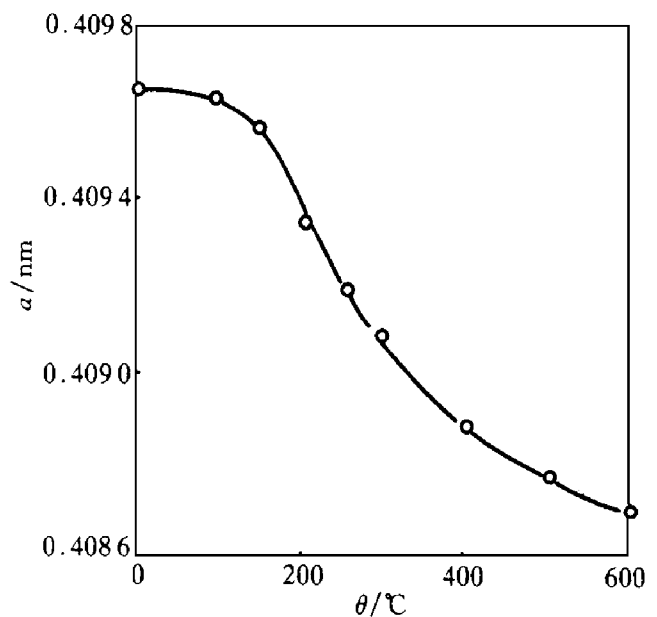


Fig. 5 Dependence of lattice parameters of RS Ag-Gd₆ alloy foil on aging temperature

above 250 °C, the precipitated particles grew up and the hardness decreased quickly.

4.2 Phase transformation in aging process

The diffraction data of Ag-Gd₄ alloy rapidly solidified and followed by aging at 400 °C are listed in Table 2. It indicated that the precipitate phase which was responsible for age hardening

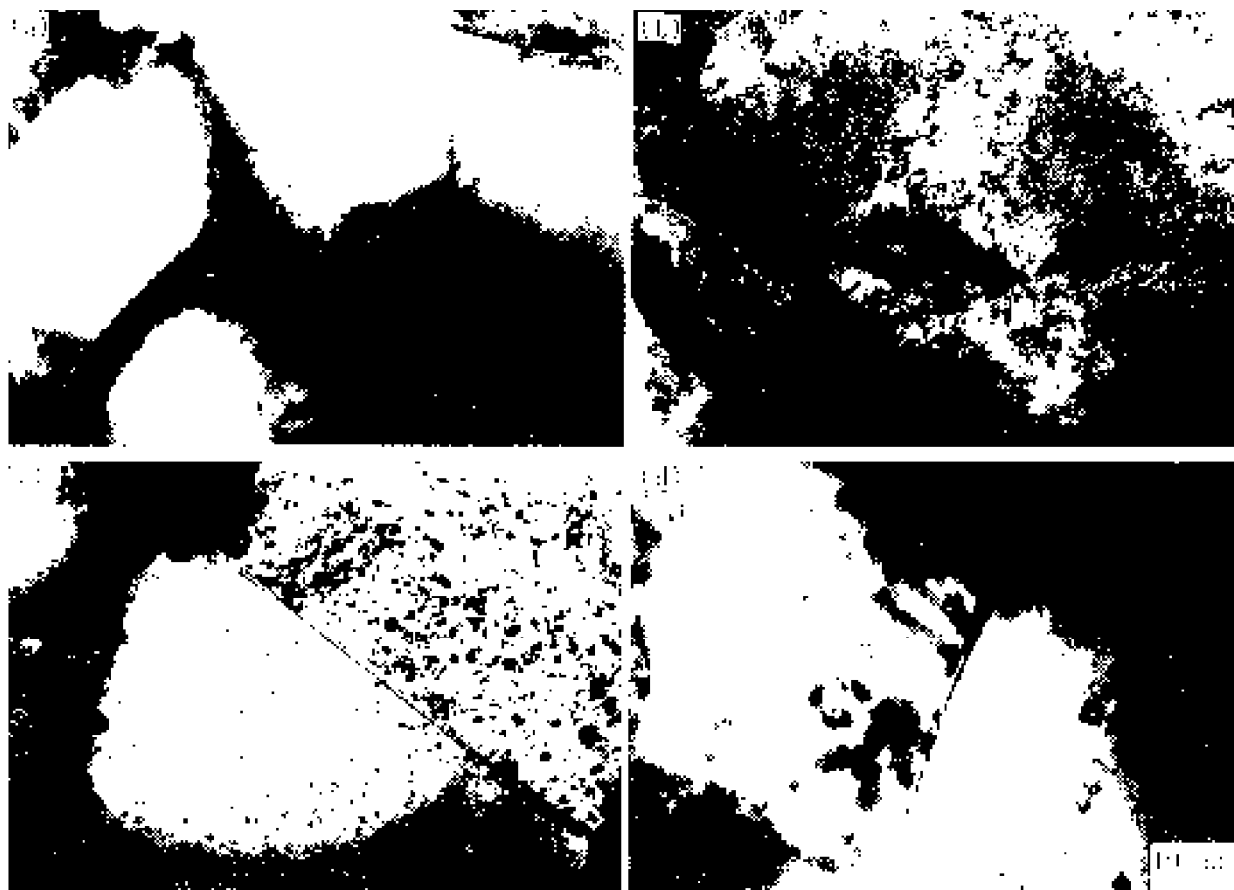


Fig. 6 Aging microstructure of RS Ag-Gd₄ alloy

(a) -150 °C; (b) -200 °C; (c) -250 °C; (d) -350 °C

Table 2 A comparison of diffraction data of Ag-Gd₄ alloy aged at 400 °C

Ag-Gd ₄ alloy aged at 400 °C			Ag ^[5]			Ag ₅₁ Gd ₄ ^[7]		
2θ/(°)	<i>d</i> _{exp} /nm	<i>I</i> / <i>I</i> ₁	<i>d</i> /nm	<i>I</i> / <i>I</i> ₁	<i>hkl</i>	<i>d</i> /nm	<i>I</i> / <i>I</i> ₁	<i>hkl</i>
28.3	0.315 1	2				0.310 0	4	212
36.12	0.248 4	4				0.248 7	100	213
37.58	0.239 1	4				0.239 2	82	410
38.1	0.236 0	100	0.235 8	100	111			
38.82	0.231 7	2				0.231 9	30	411
44.26	0.204 4	33	0.204 5	40	200			
63.16	0.147 0	1				0.147 2	8	415
64.4	0.144 5	19	0.144 5	25	220			
77.34	0.123 2	16	0.123 2	26	311			
81.48	0.118 0	6	0.118 0	12	222			
97.88	0.102 1	2	0.102 2	4	400			
110.44	0.093 7	6	0.093 8	12	331			
114.8	0.091 4	5	0.091 4	12	420			

was the $\text{Ag}_{51}\text{Gd}_{14}$ phase, and that the aged Ag-Gd alloy consisted of $\text{Ag}(\text{Gd}) + \text{Ag}_{51}\text{Gd}_{14}$, whereas the Ag_3Gd phase disappeared. The lattice parameters of the $\text{Ag}(\text{Gd})$ solid solution decreased to be 0.40886 nm at 400 °C and 0.4087 nm at 600 °C, which corresponded with values in equilibrium state at 400 and 600 °C, respectively. The results indicated that the metastable extended solid solubility restored to the equilibrium solid solubility and that supersaturated solid solution turned into equilibrium one in ageing process. $\text{Ag}_{51}\text{Gd}_{14}$ is a hexagonal structure with $a = 1.2767$ nm, $c = 0.9311$ nm and $T_m = 975$ °C and is an equilibrium intermediate phase with a homogeneous region^[3]. It indicated that the Ag_3RE metastable phase turned into the equilibrium phase $\text{Ag}_{51}\text{Gd}_{14}$.

5 DISCUSSION

Steeb *et al.*^[8-10] found at first the Ag_3RE congruent compound in Ag-Sm, Ag-Gd, Ag-Tb, Ag-Dy and Ag-Er systems. According to the recent phase diagrams^[3, 11], the equilibrium phase was the $\text{Ag}_{51}\text{RE}_{14}$ formed from melt and did not need large undercooling, and their lattice parameters were approximate to those of Ag_3RE compound. Obviously, the lattice and component of $\text{Ag}_{51}\text{RE}_{14}$ phase were related to cooling rate. In the condition of RS, the large supercooling was favourable to the formation of Ag_3RE compound as a metastable phase. Although Ag_3RE is similar to Ag_{51}RE in structure, the former is a congruent compound with stoichiometry and the latter is a compound with variable concentration of RE solute. Perhaps, the atomic clusters or crystal embryos of Ag_3RE existed in the alloy melt. The Ag_3RE embryos had not been restrained but formed Ag_3RE phase under RS condition. In the followed annealing process, the Ag_3RE phase transformed into $\text{Ag}_{51}\text{RE}_{14}$ phase by means of the composition regulation. If the cooling rate is very low or the undercooling is very small, there is enough time for the composition regulation in solidification

process, and the $\text{Ag}_{51}\text{RE}_{14}$ equilibrium phase can be formed. So, the Ag_3RE is a metastable phase as far as $\text{Ag}_{51}\text{RE}_{14}$ phase is concerned.

6 CONCLUSIONS

Two kinds of RS Ag-Gd alloy specimens, splat foils with average thickness 0.08 mm and spun ribbons with average thickness 0.03 mm were prepared by hammer-anvil and spinning techniques. The cooling rate reached 10^6 and 10^7 K/s, respectively. The solid solubility of Gd had extended to 5% and 6% from 0.95% equilibrium value. A metastable hexagonal intermediate phase, Ag_3Gd , occurred in RS Ag-Gd alloy containing Gd concentration above the metastable solid solubility limit. In following ageing process of the RS Ag-Gd alloys, the metastable supersaturated solid solubility turned to equilibrium one; the metastable phase Ag_3Gd turned to equilibrium intermediate phase $\text{Ag}_{51}\text{Gd}_{14}$. A strong solid solution and ageing strengthening response has been observed in RS Ag-Gd alloys and enhanced with increase of Gd concentration. The RS technique can be used to develop new Ag-RE alloys.

REFERENCES

- 1 Duwez P, Willens R H, Klement Jr W. J Appl phys, 1960, 31: 1136.
- 2 Jones H. J Mater Sci, 1984, 19: 1048.
- 3 Gschneidner Jr K A, Calderwood Bull F W. Alloy Phase Diagram, 1986, 6: 138.
- 4 Ning Yuantao, Zhou Xinmin, Dai Hong. Chin J Met Sci Technol, (in Chinese), 1991, 7: 391.
- 5 ASTM Card: 40-783.
- 6 ASTM Card: 23-996.
- 7 ASTM Card: 25-1147.
- 8 Steeb S, Godel D, Lohr C. J Less-Common Metals, 1968, 15: 137.
- 9 Donolato S, Steeb S. J Less-Common Metals, 1968, 18: 442.
- 10 Kiessler G, Gebhard E, Steeb S. J Less-Common Metals, 1972, 26: 295.
- 11 Gschneidner Jr K A, Calderwood Bull F W. Alloy Phase Diagram, 1986, 6: 15, 17, 142, 144.

(Edited by He Xuefeng)